Journal of Physical and Theoretical Chemistry
of Islamic Azad University of Iran, 14 (1) 1-14: Spring 2017
(J. Phys. Theor. Chem. IAU Iran)
ISSN 1735-2126

Corrosion Inhibition of 5-Methyl-2H-imidazol-4-carboxaldehyde and 1H-Indole-3-carboxyaldehyde on Mild Steel in 1.0 M HCl: Gravimetric Method and DFT Study

B. Semire*, O. F. Adekunle, S. B. Akanji and V. Adewumi

Department of Pure and Applied Chemistry, Faculty of Pure and Applied Sciences, Ladoke Akintola University of Technology, Ogbomoso, Oyo State, Nigeria

Received January 2017; Accepted July 2017

ABSTRACT

The study examined corrosion inhibition of corrosion inhibition of 5-methyl-2H-imidazol-4-carboxaldehyde and 1H-Indole-3-carboxaldehyde on mild steel in acidic medium using weight loss and Density Functional Theory (DFT) methods. DFT calculations were carried out at B3LYP/6-31+G** level of theory in aqueous medium on the molecular structures to describe electronic parameters. The values of thermodynamic parameters such as free energy of adsorption (ΔG^{o}_{ads}), adsorption equilibrium constant (K_{ads}), adsorption entropy (ΔS^{o}_{ads}), adsorption enthalpy (ΔH^{o}_{ads}) and activation energy (E_a) were calculated, analyzed and discussed. The adsorption process on mild steel surface showed that 4-methylimidazol-5-carboxaldehyde and Indole-3-carboxaldehyde obeyed Freundlich and Temkin adsorption isotherms respectively. Also, the molecular parameters associated with inhibition efficiency such as E_{HOMO}, E_{LUMO}, band gap energy (E_{LUMO}- E_{HOMO}), softness (S), electron affinity (EA) and number of electrons transfer were calculated. The higher inhibitory property of 5-methyl-2H-imidazol-4-carboxaldehyde was attributed to the presence of higher number of protonation sites as a result of higher number of nitrogen atoms, increase in number of plane protonated species and higher net charges on the ring atoms.

Keywords: 5-methylimidazol-4-carboxaldehyde; Indole-3-carboxaldehyde; Weight loss; DFT

INTRODUCTION

Corrosion is one of the major problems facing industries that are involved in the use of machine made from various metals. Concomitantly, it causes hazard to the society as well as the human population. However, different methods such as galvanization, cathode protection and recently the use of organic compounds as corrosion inhibitors have been suggested and implemented, to minimize the effect of corrosion on metals. Among the efficient corrosion inhibitors used to prevent deterioration of metals are heterocyclic organic compounds consisting of a π-electrons system [1-3]. Moreover, most effective and efficient corrosion inhibitors are organic compounds with heteroatoms and functional groups, as they are capable of facilitating the adsorption onto the metal surface [4]. However, these heterocyclic organic compounds are very important in biological reaction; they are environmental friendly, easily synthesized and purified [5]. The effectiveness of these organic

*Corresponding author: bsemire@lautech.edu.ng

compounds as corrosion inhibitors has been interpreted in terms of their molecular structures, molecular size, molecular mass, presence of hetero-atoms, electron density at the donor atoms, aromaticity and adsorptive tendencies, the frontier molecular orbital; HOMO (higher occupied molecular orbital) energy, the LUMO (lower unoccupied molecular orbital) energy, chemical potential (μ) and hardness (η), electronegativity (χ), and electron transfer number (ΔN) among others [6-11].

The corrosion inhibition efficiency (IE) of organic compounds is connected with their adsorption properties. The effect of the adsorbed inhibitor is to protect the metal from the corrosive medium [5]. To greater extent, various inhibition mechanisms have been considered regarding different situations created by changing various factors such as medium and inhibitor in the system .i.e. metal/acid medium/inhibitor [12-13]. Theoretical approaches are now becoming popular in explaining the interactions between the inhibitor molecules and the metal surface, howbeit, the recent trend is the involvement of the theoretical methods in corrosion studies [14-16].

The adsorption of the inhibitor onto the metal surface proceeds through charge transfer from the charged inhibitor's molecule to the charged metal (physical adsorption) or by electron transfer from the inhibitor molecule to the metal (chemical adsorption). In all cases, chemisorption succeeds physiosorption; therefore, corrosion inhibition process can be viewed as a process that involves electrophilic and nucleophilic attack [17-19]. Therefore, molecular reactivity descriptors such as global electrophilicity/nucleophilicity, global softness, local electrophilicity/nucleophilicity, local softness and molecular planarity have been observed to be very important parameters in the selection of effective organic inhibitors. Planar molecules are adsorbed well on metal surfaces because more of the organic molecules (inhibitors) come in contact with the metal surfaces.

The study aimed at examining the inhibitory action of 5-methyl -2H-imidazol-4-carboxaldehyde and 1H-Indole-3-carboxaldehyde (Scheme 1) toward the corrosion of mild steel in 1.0M hydrochloric acid solution using weight loss and theoretical methods (DFT). This was with a view to analyzing the effect of temperature on corrosion rate of mild steel and the inhibition efficiency of the studied molecules with the use of some thermodynamic parameters necessary for the understanding of the corrosion mechanism.

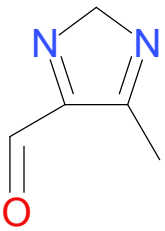

(a) 5-methyl-2H-imidazole-4-carbaldehyde

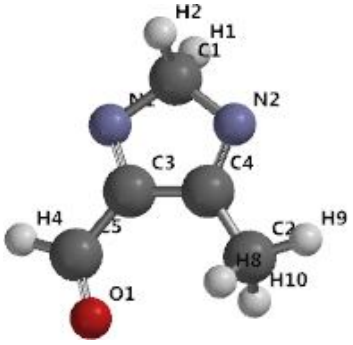

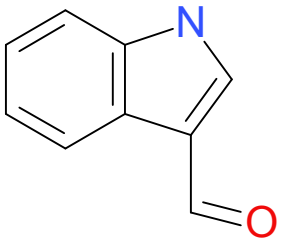

(b) 1H-indole-3-carbaldehyde

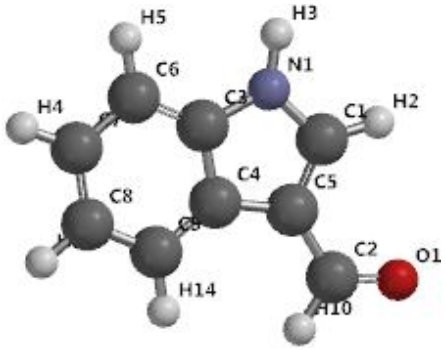

Scheme 1. Schematic and Optimized structures of the studied inhibitors with numbering of atoms.

MATERIALS AND METHODS

Experimental procedures

The carbon steel (containing 0.21% C, 0.35% Mn, 0.003% Si, 0.24% P and 99.20% Fe by mass) was mechanically press-cut into rectangular coupons of dimension 4.0 cm x 3.0 cm x 0.2 cm, grounded with SiC abrasive paper, degreased in ethanol, dried with acetone, weighed and stored in moisture free desiccators prior to usage [20]. The corrodent (acid) of 1.0M concentration was prepared from stock solution of HCl with 37% purity by serial dilution. The analytical grade (Sigma Aldrich) inhibitor (5-methyl-2H-imidazol-4-carboxaldeyhde and/or 1H-Indole-3-carboxyaldehyde) was added without further purification to the acid solution in concentration ranging from 1.0×10^{-4}µM, 0.8×10^{-4}µM, 0.6×10^{-4}µM, 0.4×10^{-4}µM and 0.2×10^{-4}µM in different beaker. The solution without inhibitor (blank) was taken as control experiment for comparison.

The gravimetric measurements were conducted under total immersion in 50ml of test solution maintained at 303K-333K. The pre-cleaned and weighed carbon steel was immersed in beakers containing the test solutions, and weight loss was determined with respect to time. The coupon was retrieved from the test solutions at 1hour interval progressively for 5 hours and immersed in 20% KOH solution, then removed and scrubbed, washed in distilled water, dried in acetone and weighed each time it been retrieved from the test solution [21].

The weight loss was taken to be the difference between the weight of coupon at a given time and its initial weight, using digital weighing balance with ± 0.001g sensitivity and the difference was used to compute the corrosion rate given by:

$\Delta W = W_1 - W_2$ which represent the weight loss.

The rate $(\rho) = \frac{\Delta W}{At}$ (1)

where, W_1 = initial weight, W_2= weight after corrosion has occured, ΔW= change in weight.

The surface area covered by the inhibitor is given by:

Surface coverage $(\theta) = \frac{(\rho 1 - \rho 2)}{\rho 1}$ - (2)

while the efficiency of the inhibitor was calculated by:

Inhibition efficiency,

$$\% I.E = \left[\frac{\rho 1 - \rho 2}{\rho 1}\right] \times 100 \quad (3)$$

where ρ1 and ρ2 are rates of corrosion in the presence and absence of inhibitor respectively.

Thermodynamic parameters for the absorption process were observed from graph using Arrhenius equation (4) and transition state equation (5). Activation parameter for the corrosion process was thus calculated from the plotted graph [20,21].

$$\rho = A\, exp\left(\frac{-E_a}{RT}\right) \quad (4)$$

$$\rho = \left(\frac{RT}{Nh}\right) exp\ \left(\frac{\Delta Sa^*}{R}\right)\ exp\ \frac{-\Delta Ha^*}{RT} \quad (5)$$

where (ρ) is the rate of corrosion for mild steel in 1.0M HCl solution, T is the absolute temperature, A is the Arrhenius factor/exponential factor, N is the Avogadro's number, R is the universal gas constant, E_a is the activation energy for the corrosion process, ΔH_a^* is the enthalpy of activation, ΔS_a^* is the entropy of activation and h is the Plank constant.

Three isotherms via Langmuir, Temkin and Freundlich were considered to determine the best fit isotherm for the corrosion inhibition of mild steel in 1.0M HCl.

Computational details

Conformation search was performed on 5-methyl-2H-imidazol-4-carboxaldehyde and 1H-Indole-3-carboxaldehyde employing semi-empirical AM1 method Monte Carlo search algorithm. For each conformational search, 1000 conformers were examined, only conformers within ±10 kJ/mol of energy window were considered. The lowest-energy conformer of this conformational search was taken for further DFT calculations [22]. All calculations were performed on the molecules with DFT of Becke's three parameter hybrid functional with correlation of Lee, Yang and Parr [23]. Optimization of molecules was performed at B3LYP/6-31+G** level of theory in gas phase [24]. Single point calculations were performed in aqueous medium at the same level of theory using optimized geometry obtained in the gas phase. The molecular descriptors calculated were chemical hardness (η), chemical softness (S), E_{HOMO} and E_{LUMO}, electronegativity (χ), electrophilicity index (ω), chemical potential (μ) and Fukui Function indices.

The conceptual DFT chemical potential is described as the first derivative of the energy with respect to the number of electrons in an external potential, which is equivalent to the negativity of the electronegativity (χ) [25,26].

$$\mu = \left(\frac{\partial E}{\partial N}\right) v(r) = -\chi = -\left(\frac{IP+EA}{2}\right) \approx -\left(\frac{E_{HOMO}+E_{LUMO}}{2}\right) \quad (6)$$

where *E* is the total energy, μ is the chemical potential, *N* is the number of electrons, and $v_{(r)}$ is the external potential of the system.

Chemical hardness (η) is defined within the DFT concept as the second derivative of the energy (*E*) with respect to (*N*) as property which measures both stability and reactivity of the molecule [27,28] and softness as $\frac{1}{\eta}$.

$$\eta = \left(\frac{\partial^2 E}{\partial N^2}\right) v(r) = (\mathrm{IP} - \mathrm{EA})/2 \approx (\mathrm{E_{HOMO}} - \mathrm{E_{LUMO}})/2 \quad (7)$$

The number of electron transfer (ΔN) when two systems (i.e. Fe and inhibitor) are in contact is:

$$(\Delta \mathrm{N}) = \frac{\mathrm{X_{Fe}} - \mathrm{X_{inh}}}{2(\eta_{Fe} + \eta_{inh})} \quad (8)$$

where X_{Fe} (taken to be 7.0eV) and X_{inh} are absolute electronegativity of the metal (Fe) and inhibitor molecule respectively, η_{Fe} (equals zero) and η_{inh} are the absolute hardness of Iron and the inhibitor molecule

respectively.

The electrons flow from lower electronegative χ (inhibitor) to higher electronegative χ (Fe), until the chemical potentials becomes equal [28, 29]. Fukui Functions was used to evaluate local reactivity indices as shown in equations 9 and 10;

$f^{+}_{(r)} = P_{N+1(r)} - P_{N(r)}$ (for nucleophilic attack) (9)

$f^{-}_{(r)} = P_{N(r)} - P_{N-1(r)}$ (for electrophilic attack) (10)

where $P_{N+1(r)}$, $P_{N(r)}$ and $P_{N-1(r)}$ are the electronic densities of anionic, neutral and cationic species respectively [29].

RESULT AND DISCUSSION

The efect of temperature on the rate of corrosion

The corrosion parameters such as weight loss (ΔW), corrosion rate (ρ), area coverage (θ) and inhibition efficiency (I.E) for mild steel in 1.0M HCl solution in the presence and absence of inhibitor increase with increasing temperature as shown in Table 1. Although, various factors influence the corrosion rate of metals, temperature has been considered as one of the principal factor that increases the rate of corrosion and aggravates the deterioration of metal components [30,31]. Weight loss and corrosion rate increase with increasing temperature either in uninhibited system (blank) or inhibited system (in the presence of 5-methyl-2H-imidazol-4-carboxaldehyde or 1H-Indole-3-carboxaldehyde) but decreases with increasing inhibitor concentration at a specific temperature (Table 1).

The inhibition efficiency at a specific concentration decreases with increasing temperature due to desorption of inhibitor from metal surface, which is associated with increase in temperature (i.e. temperature is inversely correlated to the rate of corrosion on metal surface). The rate of corrosion of iron in the presence of 1H-Indole-3-carboxaldehyde (B) is slightly higher than the rate of corrosion in the presence of 5-methyl-2H-imidazol-4-carboxaldehyde (A) at a specific concentration. At 6.0×10^{-5}M concentration of inhibitor, the corrosion rates are 2.52×10^{-5} and 2.81×10^{-5}gcm^{-2}min^{-1} for A and B respectively at 303K, whereas the rates are 10.09×10^{-5} and 10.26×10^{-5} gcm^{-2}min^{-1} for A and B respectively at 333 K (Table 1). This suggests that 5-methyl-2H-imidazol-4-carboxaldehyde (A) is a better corrosion inhibitor than (B) which may due to the presence of higher number of nitrogen atoms [32] thus making it better adsorbed on to the metal surface by interaction between the lone pairs of electrons of inhibitor nitrogen atoms and the metal surface [33].

The effect of concentration on the rate of corrosion.

Important information about the interaction between the inhibitor and steel surface can be provided by the adsorption isotherm. In this work, it is established that surface coverage (θ) increases with increasing inhibitor concentration, which is attributed to more adsorption of inhibitor molecules onto the metal surface [34]. The corrosion rate (gcm^{-2}min^{-1}) depends on the concentration of inhibitor (5-methyl-2H-imidazol-4-carboxaldehyde and 1H-Indole-3-carboxyaldehyde) in 1.0M HCl acid solution at 303K-333K as shown in Table 1. The corrosion rate of the mild steel in the acid solution decreases with increasing concentration of the inhibitor; thus suggesting that 5-methyl-2H-imidazol-4-carboxaldehyde and 1H-Indole-3-carboxaldehyde can be used as corrosion inhibitors for mild steel in HCl acid solution. At 303K, it is observed that the rate of corrosion decreases appreciably from 3.06×10^{-5} to 1.70×10^{-5} and 3.05×10^{-5}

to 2.02×10^{-5} $gcm^{-2}min^{-1}$ for inhibitors A and B respectively as inhibitor concentration increases from 0.2×10^{-4} to 1.0×10^{-4}M.

It is a well-known fact that increases in concentrations of an inhibitor lowers the rate of corrosion by increasing the surface coverage area of the inhibitor on the metal surface [35]. At specific temperature, the surface coverage (θ) of the inhibitor on metal surface increases with increasing concentration of the inhibitor, this is observed in the systems containing inhibitors A and B. However, larger surface coverage is observed with inhibitor (A) which has been attributed to the number of nitrogen atoms that facilitates adsorption of A on metal surface [32, 33].

Table1. Experimental data for the corrosion of mild steel in 1.0M HCl in the absence and presence of 5-methyl-2H-imidazol-4-carboxaldehyde (A) and 1H-Indole-3-carboxaldehyde (B)

Conc. / Temp.			Blank	2.0 x10^{-5} Mol/dm^3	4.0 x10^{-5} Mol/dm^3	6.0 x10^{-5} Mol/dm^3	8.0 x10^{-5} Mol/dm^3	1.0 x10^{-4} Mol/dm^3
303K	ΔW	A	0.054	0.036	0.033	0.029	0.026	0.020
		B		0.019	0.018	0.017	0.016	0.013
	P ×10^{-5}	A	4.590	3.060	2.750	2.522	2.253	1.701
		B		3.051	2.922	2.811	2.621	2.023
	Θ	A	-	0.333	0.401	0.451	0.509	0.630
		B	-	0.341	0.363	0.391	0.431	0.515
	I.E%	A	-	33.33	40.09	45.10	50.98	62.96
		B	-	34.10	36.32	39.12	43.10	51.51
313K	ΔW	A	0.073	0.059	0.052	0.046	0.043	0.036
		B		0.038	0.037	0.032	0.030	0.026
	P ×10^{-5}	A	6.210	4.912	4.354	3.971	3.602	3.041
		B		4.845	4.583	4.122	3.841	3.460
	Θ	A	-	0.209	0.299	0.361	0.420	0.510
		B	-	0.223	0.262	0.342	0.384	0.443
	I.E%	A	-	20.93	29.95	36.07	42.02	51.04
		B	-	22.33	26.24	34.21	38.43	44.31
323K	ΔW	A	0.103	0.088	0.081	0.077	0.069	0.062
		B		0.071	0.068	0.063	0.058	0.052
	P ×10^{-5}	A	8.501	7.404	6.890	6.382	5.870	5.271
		B		7.313	6.972	6.463	5.953	5.361
	Θ	A	-	0.129	0.189	0.249	0.310	0.380
		B	-	0.142	0.181	0.238	0.295	0.365
	I.E%	A	-	12.94	18.94	24.93	31.00	38.01
		B	-	14.21	18.10	23.81	29.52	36.51
333K	ΔW	A	0.136	0.131	0.131	0.121	0.113	0.104
		B		0.110	0.116	0.120	0.124	0.126
	P ×10^{-5}	A	11.601	10.913	10.441	10.092	9.631	8.934
		B		10.861	10.482	10.263	9.658	9.165
	Θ	A	-	0.060	0.102	0.130	0.170	0.230
		B	-	0.049	0.099	0.113	0.161	0.209
	I.E%	A	-	6.04	10.20	13.02	16.98	23.02
		B	-	4.90	9.90	11.32	16.13	20.85

For instance, the surface coverage (θ) are 0.451, 0.509 and 0.630 at 303K for A; and 0.391, 0.431 and 0.515 for B at 303K with 0.6×10^{-4}M, 0.8×10^{-4}M and 1.0×10^{-4}M inhibitor's concentration respectively.

Thermodynamic activation parameters

The activation energy (E_a) for blank and optimum concentration of 5-methyl-2H-imidazol-4-carboxaldehyde and 1H-Indole-3-carboxaldehyde were determined from Arrhenius plot (equation 4). Figure 1 shows that the linear regression coefficient for each molecule is close to one, implying that mild steel corrosion in 1.0M HCl could be studied using kinetic model. The E_a value for the corrosion of the metal in the solution that contains the inhibitor is higher compare to that in the uninhibited system (blank) as shown in Table 2. The E_a calculated for corrosion of iron in acidic solution containing 5-methyl-2H-imidazol-4-carboxaldehyde (A) and 1H-Indole-3-carboxaldehyde as inhibitors (B) are 45.943 and 39.117 kJ/mol respectively against 25.732 kJ/mol for the uninhibited system (blank). This implies that adsorption occurs on the metal surface for the inhibited system (using 1.0×10^{-4} M as optimum concentration), and also shows that 5-methyl-2H-imidazol-4-carboxaldehyde (A) has a superior corrosion inhibitory ability.

ΔS_a^* and ΔH_a^* were calculated from equation (5), the plot of ln(ρ/T) against 1/T shows a linear graph with $\Delta H_a^*/R$ as slope, and $\ln(R/Nh) + \Delta S_a^*/R$ as intercept (Figure 2). The enthalpy and entropy were evaluated for blank and optimum concentration from the plot. ΔH_a^* and ΔS_a^* for the dissolution reaction in the presence of inhibitor are higher than in the absence of inhibitor (blank) (Table 2). The ΔH_a^* calculated for the dissolution reaction are 43.324, 26.986 and 23.113 kJ/mol for inhibitor A, inhibitor B and blank respectively. The positive sign for ΔH_a^* reflects the endothermic nature of the steel dissolution process, suggesting that the dissolution of mild steel is slow in the presence of inhibitor. The higher ΔH_a^* value for inhibitor A shows that more energy is required for corrosion to occur in the presence of 5-methyl-2H-imidazol-4-carboxaldehyde than in 1H-Indole-3-carboxaldehyde, this means that corrosion occurred more slowly in the presence of inhibitor A; thus enhancing inhibition efficiency. The large negative value of ΔS_a^* implies that the activated complex is the rate determining step, rather than the dissociation step. The value of ΔS increases in the presence of inhibitor (Table 2), suggesting that there is an increase in the disorderliness as the reactants are converted into the activated complexes [30].

Table 2. Activation parameters for mild steel in 1.0M HCl solution for blank and optimum concentration of inhibitors A and B.

Inhibitor concentration		Corrosion Rate	R^2	E_a (kJ/mol)	ΔS_a^* (J/mol)	ΔH_a^* (kJ/mol)
Blank		4.59×10^{-5}	0.999	25.732	-251.834	23.113
1.0×10^{-4}M	A	1.70×10^{-5}	0.999	45.943	-193.258	43.324
	B	2.20×10^{-5}	0.988	39.117	-234.000	26.986

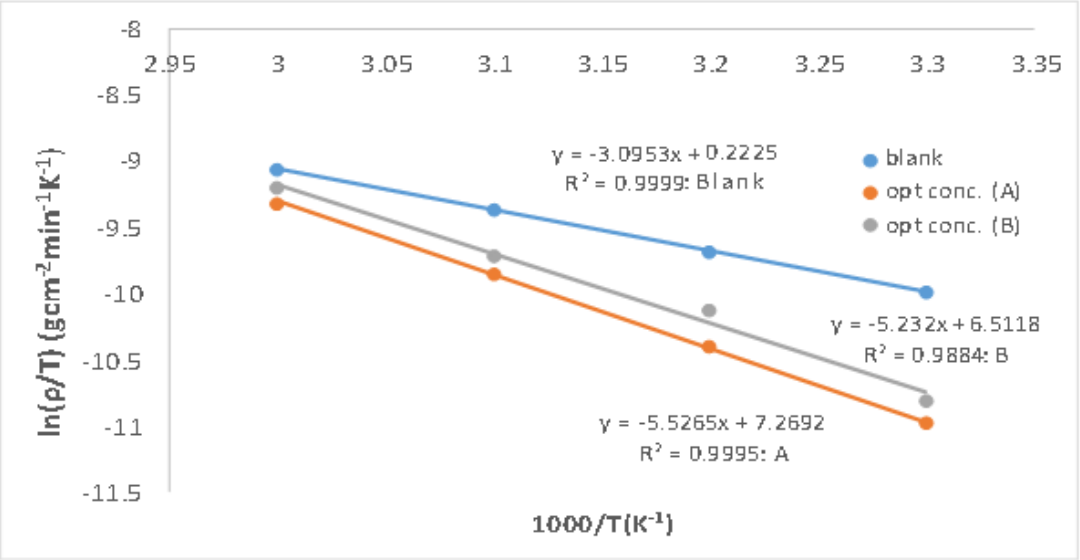

Fig. 1. Graph of ln (ρ/T) against 1000/T (K^{-1}) at blank and optimum concentration for A and B

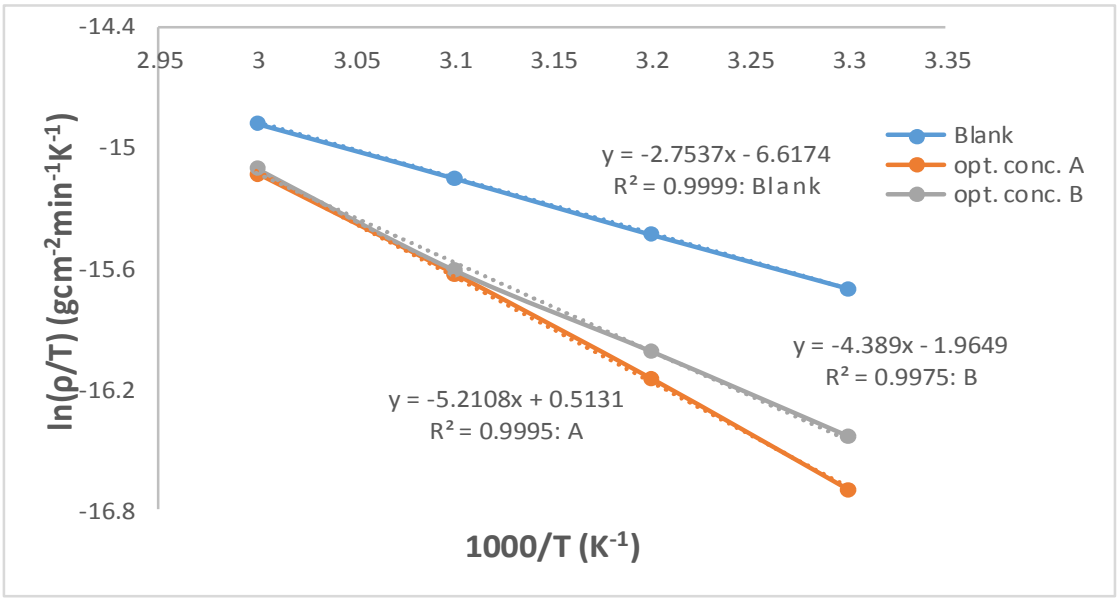

Fig. 2. Transition state graph of ln (ρ/T) against 1/T for blank and optimum concentration for A and B

Adsorption isotherms and thermodynamic parameters

Basic information on the interaction between the inhibitor and the metal surface can be provided by the adsorption isotherm, which depends on the degree of electrode surface coverage, θ [34]. A good organic inhibitor tends to accept electron(s) from the d-orbital shell of the metal, and also donate electron(s) to the d-orbital shell of the metal thereby creating a system of forward and backward reaction called feedback reaction [3, 30, 33] until a quasi-equilibrium state is established.

Therefore, it is reasonable to consider the quasi-equilibrium adsorption using the appropriate equilibrium isotherms. In this paper, three different isotherms are considered via Langmuir, Temkin and Freundlich isotherms to understand the adsorption process. The isotherm with the lowest adsorption constant (K_{ads}) and highest regression value is taken as the best fit isotherm for the adsorption process.

The estimated K_{ads}, slope and R^2 values for Langmuir, Freundlich and Temkin adsorption isotherms are listed in Table 3 as well as the free energy (ΔG_{ads}) values for the isothermic adsorption processes derived from equation (11):

$$\Delta G_{ads} = -R\,T\,ln\,(55.5\,K_{ads}) \qquad (11)$$

where R is the universal gas constant, T is the thermodynamic temperature and the value of 55.5 is the concentration of water in the solution. The negative value calculated for ΔG_{ads} indicates spontaneous adsorption of the inhibitor onto the mild steel surface as well as the strong interaction between the inhibitor molecule and the metal surface [36, 37].

In general, when $\Delta G_{ads} \leq$ -20 kJ/mol, it is considered to be interactions between the charged molecules and the metal (physisorption), while those around -40 kJ/mol or higher are associated with chemisorption as a result of transfer or share of electrons from organic molecules to the metal surface to form a coordinate bond [36]. The calculated ΔG_{ads} values for inhibitors A and B are -37.374 and -35.685 kJ/mol for Langmuir; -6.962 and -13.208 kJ/mol for Freundlich; and -10.750 and -10.834 kJ/mol for Temkin respectively (Table 3). However, the best fit isotherm is Freundlich for inhibitor A and Temkin for inhibitor B. The calculated ΔG_{ads} for both inhibitors A and B are less than -20 kJ/mol in each case; therefore, the adsorption mechanism of 5-methyl-2H-imidazol-4-carboxaldehyde (A) and 1H-Indole-3-carboxaldehyde (B) on mild steel in 1.0M HCl solution could be considered as a typical physisorption.

Molecular descriptors for inhibitors A and B

The frontier molecular orbitals and Fukui functions for 5-methyl-2H-imidazol-4-carboxaldehyde (A) and 1H-Indole-3-carboxaldehyde (B) calculated in aqueous medium at B3LYP/6-31+G** were used to analyze the reactivity of the studied molecules. The highest occupied molecular orbital (HOMO) and the lowest unoccupied molecular orbital (LUMO) are related to the electron donating and accepting ability of a molecule respectively. Organic inhibitors with high HOMO energy (E_{HOMO}) have high electrons donating energy (E_{LUMO}). Increase in the HOMO energy increases binding ability of the inhibitor to the metal surface thereby facilitating adsorption, thus enhancing the inhibition efficiency of the molecule [1]. However, the E_{HOMO}, E_{LUMO}, dipole moment, softness (S) and number of

Table 3. Thermodynamic parameters for the adsorption of 5-methyl-2H-imidazol-4-carboxaldehyde (A) and 1H-Indole-3-carboxaldehyde (B) in 1.0M HCl acid solution

Isotherms		Regression coefficient (R^2)	Free energy (ΔG_{ads} in kJ/mol)	K_{ads} (M^{-1})	Slope
Langmuir	A	0.921	-37.374	50000	1.593
	B	0.936	-35.685	25000	1.705
Freundlich	A	0.988	-6.962	0.2858	0.066
	B	0.944	-13.208	3.3728	0.045
Temkin	A	0.971	-10.750	1.2853	0.071
	B	0.994	-10.834	1.3218	0.043

electrons transfer (ΔN) for inhibitor A are -7.82 eV, -2.93 eV, 1.35 Debye, 0.2342 eV^{-1} and 0.166 respectively. In order to predict the preferred conformation of inhibitor A in aqueous medium, calculations were also performed on possible protonated structures of the inhibitor A at B3LYP/6-31+G** in aqueous medium. The calculated E_{HOMO}, E_{LUMO}, dipole moment, softness (S) and number of electrons transfer (ΔN) are -8.31 eV, -4.19 eV, 1.92 Debye, 0.243 eV^{-1} and 0.091 for protonation at N1; -7.98 eV, -3.48 eV, 8.11 Debye, 0.222 eV^{-1} and 0.141 for protonation at N2; and -8.74 eV, -4.86 eV, 8.36 Debye, 0.258 eV^{-1} and 0.026 for di-protonation at N1, N2 respectively (Table 4). Therefore, higher E_{HOMO} coupled with higher number of electron transferred in neutral inhibitor A will facilitate the flow of electrons from the lower electronegativity of the inhibitor A to the higher electronegativity iron surface (Table 4).

Similarly, the E_{HOMO}, E_{LUMO}, diploe moment, softness (S) and number of electrons transfer (ΔN) for inhibitor B are also considered to guess the preferred conformation in aqueous medium. The calculated E_{HOMO}, E_{LUMO}, dipole moment, softness (S) and ΔN for inhibitor B are -6.29 eV, -1.81 eV, 6.27 Debye, 0.223 eV^{-1} and 0.329 respectively. For protonation, the E_{HOMO}, E_{LUMO}, dipole moment, softness (S) and number of electrons transfer (ΔN) are -6.99 eV, -2.83 eV, 8.60 Debye, 0.240 eV^{-1} and 0.251 for protonation at N (keto form); and -6.73 eV, -2.84 eV, 6.74 Debye, 0.257 eV^{-1} and 0.285 for protonation at N (enol form) respectively (Table 5). Correspondingly, higher E_{HOMO} and higher value of ΔN for neutral inhibitor B will ease the flow of electrons from the lower electronegativity of the inhibitor to the higher electronegativity iron surface. However, the presence of protonated forms of inhibitors A and B with lower E_{LUMO} and higher softness in aqueous medium will increase the inhibitors ability to accept electron from d-orbital of iron until the chemical potentials are equalized in aqueous medium [30, 33].

Table 4. Total Energy, Electron transfer, Softness and Hardness for inhibitor A

Molecular parameter	Neutral	Protonation at N1	Protonation at N2	Di-protonation at N1, N2
Total energy (au)	-378.870732	-379.297313	-379.308202	-379.723737
E_{HOMO} (eV)	-7.82	-8.31	-7.98	-8.74
E_{LUMO} (eV)	-2.93	-4.19	-3.48	-4.86
Dipole moment (Debye)	1.25	1.92	8.11	8.36
E_{HOMO}-E_{LUMO} (eV)	4.89	4.12	4.50	3.88
η	2.45	2.06	2.25	1.94
Softness	0.205	0.243	0.222	0.258
μ	-5.375	-6.250	-5.73	-6.80
Δn	0.166	0.091	0.141	0.026

Table 5. Total Energy, Electron transfer, Softness and Hardness for inhibitor B

Molecular parameter	Neutral	Protonated at N (ketone form)	Protonated tautomer at N (enol form)
Total energy (au)	-477.179693	-477.577147	-477.607418
E_{HOMO} (eV)	-6.29	-6.99	-6.73
E_{LUMO} (eV)	-1.81	-2.83	-2.84
Dipole moment (Debye)	6.27	8.60	6.74
E_{HOMO} - E_{LUMO} (eV)	4.48	4.16	3.89
η	2.24	2.08	1.945
Softness	0.223	0.240	0.257
μ	-4.05	-4.91	-4.785
Δn	0.329	0.251	0.285

Some of other important parameters (if other things being equal, because the nature of inhibitor interaction and efficiency may dependent on the chemical, mechanical and structural characteristics of iron surface layer) to measure the reactivity of an organic inhibitor towards adsorption on the metal surface are low energy band gap, high softness, high dipole moment and number of electrons transfer of the organic inhibitor. Comparison of the calculated molecular parameters for inhibitors A and B reveals that inhibitor B has lower energy band gap, ΔE ($\Delta E = E_{LUMO}–E_{HOMO}$); higher softness and higher dipole moment compare to inhibitor A. Decreasing in ΔE of the molecule has been attributed to increasing %IE of the molecule, because lesser/lower energy is required to remove an electron from the last occupied orbital [38]. Also, a molecule with a low energy gap is usually more polarizable with high chemical activity, low kinetic stability and high softness value [39, 40]; thus inhibitor B is expected to have higher % I.E as mentioned earlier. However, inhibitor A presents higher % I.E (%I.E = 62.96) against %I.E = 51.50 for inhibitor B. Higher % I.E of inhibitor A may be due to: (1) presence of higher number of protonation sites as a result of higher number of nitrogen atoms [32], hence increase in number of electrostatic sites and (2) increase in number of plane protonated species in addition to neutral specie (Tables 4 and 5) in aqueous medium as well as lower E_{LUMO} (E_{LUMO} = -2.93, -4.19, -3.48 and -4.86 eV for neutral, protonation at N1, protonation at N1 and di-protonations respectively); this enhances the ability of inhibitor A to accept electrons from d-orbital of iron than inhibitor B [18].

The Mullikan population charge analysis has been a useful parameter to estimate the adsorption centers of inhibitors. The Mullikan charges on N1 and N2 for neutral inhibitor A are -0.329 and -0.366*e* respectively. For neutral inhibitor B, Mullikan charge on the only nitrogen atoms is -0.462*e*. It is generally agreed that the more negatively charged a heteroatom, the more it can be adsorbed on the metal surface [10], but presence of two nitrogen atoms in inhibitor A enhances adsorption of inhibitor A on the metal surface. Another parameter that influences higher % I.E of the inhibitor A is higher total electronic charges on ring atoms. The sum of electronic charges on ring atoms are -1.858 and -0.858*e* for inhibitors A and B respectively, which correspond to the observed % I.E for the inhibitors [41]. Therefore, adsorption processes of the inhibitors on metal surface are strongly aided by electrostatic interactions in terms of π-cationic and n-cationic interactions. This indicates the process of adsorption is mainly physisorption which degreed with calculated free energy of adsorption.

Fukui indices are additional useful parameters to pinpoint the local sites for either electrophilic or nucleophilic attacks on the inhibitors. These are calculated for the neutral inhibitors using natural and Mullikan charges as shown in Tables 6 and 7. The f^- measures reactivity of an atom with respect to electrophilic attack (i.e. the characteristic of the molecule to donate electrons) and f^+ measures reactivity related to nucleophilic attack (i.e. the propensity of the molecule to accept electrons). The local reactivity calculated for inhibitor A by means of condensed Fukui functions using neutral charge population shows that the most probable sites for nucleophilic and electrophilic attacks are on C1 (0.028) and C2 (0.013) respectively. However, using Mulliken charge population analysis for local reactivity calculated for inhibitor A shows reversal of centers (i.e. C2 and C1 are possible sites for nucleophilic and electrophilic attacks respectively (Table 6)). For inhibitor B, C8 and C9 are predicted as possible sites for nucleophilic and electrophilic attacks respectively using Mulliken charge population analysis; however, C5 is predicted as a center for both nucleophilic and electrophilic sites using natural charge population analysis (Table 7).

Table 6. Fukui indices for nucleophilic and electrophilic sites on inhibitor A calculated using Natural and Mullikan electronic charges.

	Natural Charges					Mullikan Charges				
Atom	**$qN_{(r)}$**	**$qN+1_{(r)}$**	**$qN-1_{(r)}$**	**f^+**	**f^-**	**$qN_{(r)}$**	**$qN+1_{(r)}$**	**$qN-1_{(r)}$**	**f^+**	**f^-**
N1	-0.370	-0.588	-0.268	-0.218	-0.102	-0.329	-0.371	-0.237	-0.042	-0.092
N2	-0.451	-0.552	-0.319	-0.101	-0.132	-0.370	-0.366	-0.369	0.004	-0.001
C1	-0.174	-0.146	-0.183	**0.028**	0.009	-0.264	-0.290	-0.523	-0.026	**0.259**
C2	-0.728	-0.719	-0.741	0.009	**0.013**	-0.876	-0.478	-0.981	**0.398**	0.105
C3	0.078	-0.053	0.093	-0.131	-0.015	0.464	0.428	0.241	-0.036	0.223
C4	0.220	0.207	0.255	-0.013	-0.035	0.378	-0.050	0.678	-0.428	-0.300
C5	0.397	0.228	0.433	-0.169	-0.036	-0.052	-0.398	0.465	-0.346	-0.517
H1/H2	0.287	0.218	0.321	-0.069	-0.034	0.270	0.202	0.297	-0.068	-0.027
H4	0.192	0.131	0.364	-0.061	-0.172	0.245	0.151	0.419	-0.094	-0.174
H8	0.274	0.263	0.291	-0.011	-0.017	0.254	0.254	0.279	0.000	-0.025
H9	0.265	0.252	0.292	-0.013	-0.027	0.242	0.262	0.279	0.020	-0.037
H10	0.274	0.263	0.291	-0.011	-0.017	0.254	0.254	0.242	0.000	0.012
O	-0.552	-0.723	-0.146	-0.171	-0.406	-0.486	-0.599	-0.087	-0.113	-0.399

Table 7. Fukui indices for nucleophilic and electrophilic sites on inhibitor B calculated using Natural and Mullikan electronic charges.

	Natural Charges					Mullikan Charges				
atom	**$qN_{(r)}$**	**$qN+1_{(r)}$**	**$qN-1_{(r)}$**	**f^+**	**f^-**	**$qN_{(r)}$**	**$qN+1_{(r)}$**	**qN-1(r)**	**f^+**	**f^-**
N	-0.538	-0.592	-0.461	-0.054	-0.077	-0.419	-0.462	-0.343	-0.043	-0.076
C1	0.066	-0.155	0.134	-0.221	-0.068	-0.028	-0.753	-0.055	-0.725	0.027
C2	0.389	0.119	0.384	-0.27	0.005	-0.524	-1.408	-0.611	-0.884	0.087
C3	0.128	0.122	0.126	-0.006	0.002	0.323	0.504	0.366	0.181	-0.043
C4	-0.083	-0.105	-0.084	-0.022	0.001	0.337	-0.108	0.583	-0.445	-0.246
C5	-0.267	-0.266	-0.697	**0.001**	**0.430**	0.393	0.078	0.700	-0.315	-0.307
C6	-0.257	-0.280	-0.128	-0.023	-0.129	-0.403	-0.345	-0.297	0.058	-0.106
C7	-0.245	-0.259	-0.135	-0.014	-0.110	0.014	0.813	-0.027	0.799	0.041
C8	-0.253	-0.28	-0.240	-0.027	-0.013	-0.378	0.622	-0.469	1.000	**0.091**
C9	-0.229	-0.245	-0.066	-0.016	-0.163	-0.697	0.793	-0.262	**1.490**	-0.435
H2	0.271	0.230	0.300	-0.041	-0.029	0.263	0.183	0.294	-0.08	-0.031
H3	0.473	0.448	0.498	-0.025	-0.025	0.507	0.497	0.527	-0.01	-0.020
H4	0.257	0.253	0.283	-0.004	-0.026	0.218	0.247	0.248	0.029	-0.030
H5	0.259	0.251	0.287	-0.008	-0.028	0.232	0.249	0.270	0.017	-0.038
H9	0.256	0.250	0.282	-0.006	-0.026	0.212	0.234	0.232	0.022	-0.020
H10	0.168	0.098	0.192	-0.070	-0.024	0.189	0.093	0.227	-0.096	-0.038
H14	0.251	0.241	0.279	-0.010	-0.028	0.202	0.186	0.253	-0.016	-0.051
O	-0.640	-0.829	-0.553	-0.189	-0.087	-0.638	-0.834	-0.637	-0.196	-0.001

CONCLUSION

- In the present study, the corrosion inhibitory performance of 5-methyl-2H-imidazol-4-carboxaldehyde and 1H-Indole-3-carboxaldehyde on mild steel in 1.0MHCl has been studied using weight-loss method complemented by quantum chemical calculations.
- The inhibitor efficiency increases with the increasing inhibitor concentration, but at specific concentration, 5-methyl-2H-imidazol-4-carboxaldehyde is more efficient as corrosion inhibitor than 1H-Indole-3-carboxaldehyde.
- The adsorption of the two inhibitors shows that 5-methyl-2H-imidazol-4-carboxaldehyde and 1H-Indole-3-carboxaldehyde follow the Freundlich and Temkin isotherms respectively.
- The mode of adsorption of the inhibitors on metal surface is typical physisoption ($\Delta G_{ads} \leq$ -20 kJ/mol) which is supported by information derives from quantum chemical calculations.
- The higher corrosion inhibitory efficiency of 5-methyl-2H-imidazol-4-carboxaldehyde is attributed to the presence of higher number of protonation sites as a result of higher number of nitrogen atoms, increase in number of plane protonated species and higher net charges on the ring atoms.

REFERENCES

[1] P. Udhayakala, T.V. Rajendiran and S. Gunasekaran, J. of Adv. Sci. Res., 3 (2) (2012) 37-44.

[2] P. Udhayakala, T.V. Rajendiran and S. Gunasekaran, J. Comput. Methods Mol. Des., 2 (2012) 1-15.

[3] M.K. Mwadham, C.M. Lutendo, O. Muzaffer, K. Faruk, D. Ilyas, I.B. Obot, and E.E. Eno, Int. J. Electrochem. Sci., 7 (2012) 5035 – 5056.

[4] K.F. Khaled, Cor. Sci., 52 (2010) 3225-3234.

[5] O. E. Nnabuk, I.I. Benedict, E. I. Nkechi, and E. E. Eno, Int. J. Electrochem., Sci. 6 (2011) 1027 – 1044.

[6] C. Hui, F. Zhenghao, S. Wenyan, and X. Qi, Int. J. Electrochem. Sci., 7 (2012) 10121 - 10131.

[7] I. Dehri and M. Ozcan, Mater. Chem and Phys., 98 (2006) 316.

[8] M.G. Hosseini, M. Ehteshamzadeh, and T. Shahrabi, Electrochim Acta., 52 (2007) 3680.

[9] M.M. El-Naggar, Corros. Sci., 49 (2007) 2226.

[10] G. Zhang and C.B. Musgrave, Journal of Physical Chemistry A., 111(8) (2007) 1554–1561.

[11] G. Bereket, E. Hur, and C. Ogretir, Journal of Molecular Structure: THEOCHEM, 578 (2002) 79–88.

[12] J. Vosta and J. Eliasek, Corrosion Science, 11 (1971) 223–229.

[13] E.E. Eno, A. Taner, K. Fatma, L. Ian, O. Cemil, S. Murat, and A.U. Saviour, Int. J. of Quantum Chem., 110 (2010) 2614–2636.

[14] A.K. Dubey and G. Singh, Portugaliae Electrochimica Acta., 25 (2007) 221-235.

[15] N. Sally, L. Susana, N. Subramanya, and A. Ray, Mentzer M., 31 (2013).

[16] I. Ahamad, R. Prasad, E.E. Ebenso and M.A. Quraishi, Int. J. of Electrochemica Sci., 7 (2012) 3436 – 3452.

[17] V.S. Sastri, and J.R. Perumareddi, Corrosion science, 53 (1997) 617.

[18] B. Semire and A.O. Odunola, Khimiya, 22(6) (2013) 893-906; M. O. Abdulazeez, A. K. Oyebamiji and B. Semire, Lebanese Sci. J., 17(2) (2016) 217-232.

[19] B. Gomez and N.V. Likhanova, J. Phys. Chem. B., 110 (2006) 8928.
[20] I. Ahamad, R. Prasad, and M.A. Quraishi, Corros. Sci., 52 (2010) 933.
[21] J. Fang, and J. Li, J. Mol. Struct. (Theochem)., 593 (2002) 179.
[22] N.O. Obi-Egbedi, K.E. Essien, I.B. Obot, E.E. Ebenso, Int. J. of Electrochemica Sci., 6 (2012) 913-930.
[23] Spartan '14 user's guide, Wave function, Inc, Irvine, CA 92612 USA (2014)
[24] A.D. Becke, J. Chem. Phys., 98 (1993) 5648.
[25] C. Lee, W.T. Yang, and R.G. Parr, Phys. Rev. B., 37 (1988) 785.
[26] Z. Zhou and H.V. Navangul, J. Phys. Org. Chem., 3 (1990) 784-788.
[27] T. Koopmans, Physica. 1 (1934) 104-113.
[28] L. R. Domingo, M. Aurell, M. Contreras, and P. Perez, J. Phys. Chem. A., 106 (2002) 6871-6876.
[29] W. Yang, and R. Parr, Proc. Nat. Acad. Sci. USA. 82 (1985) 6723–6726.
[30] P. Udhayakala, A. Jayanthi, T.V. Rajendiran, Der Pharma Chemica., 3(6) (2011) 528-539.
[31] E.E. Eno, A.I. David and O.E. Nnabuk, Int. J. Mol. Sci., 11 (2010) 2473-2498.
[32] A. Singh, I. Ahamad, V.K. Singh, M.A. Quraishi, J. Solid State Electrochem., 15 (2011) 1087.
[33] H.L. Wang, R.B. Liu, J. Xin, Corros Sci., 46(10) (2004) 2455-2466; A.Y. El-Etre, Mater. Chem. Phys., 108 (2008) 278.
[34] S.P. Niketan, J. Smita and N.M. Girishkumar, Acta Chim. Slov., 57 (2010) 297–304.
[35] J. Sutiana, A.A. Ahmed, K. Abdulhadi, H.K. Abdul Amir and M. Abu Bakar, int. J. Mol. Sci., 14(6) (2013) 11915-11928.
[36] L. Pengju, F. Xia, T. Yongming, S. Chunning, and Y. Cheng, Mat. Sci. and App. 2 (2011) 1268-1278.
[37] H.E El Sayed, E. Ahmed, A.E. Samy, and R. Safaa, General Papers ARKIVOC., (xi) (2006) 205-220.
[38] I. Fleming, New York: John Wiley & Sons (1976).
[39] A. Ghazoui, R. Saddik, N. Benchat, M. Guenbour, B. Hammouti, S.S. Al-Deyab and A. Zarrouk, Intern. J. Electrochem. Sci., 7 (2012) 7080 – 7097.
[40] I. Lukovits, E. Kalman and F. Zucchi, Corrosion Science, 57 (2001) 3-8.
[41] K. Babic-Samardzija, K.F. Khaled and N. Hackerman, Anti-Corrosion Methods and Materials, 52(1) (2005) 11–21.